SMOOTHED PARTICLE HYDRODYNAMICS MODEL FOR REACTIVE TRANSPORT AND MINERAL PRECIPITATION

A. TARTAKOVSKY[1], T. SCHEIBE[1], G. REDDEN[2], P. MEAKIN[2], Y. FANG[1].

[1]*Pacific Northwest National Laboratory, P.O. Box 999, Richland, WA 99352;*
[2]*Idaho National Laboratory, P.O. Box 1625, MS 2025, Idaho Falls, Idaho, 83415-2025.*

ABSTRACT

A new Lagrangian particle model based on smoothed particle hydrodynamics was used to simulate pore scale precipitation reactions. The side-by-side injection of reacting solutions into two halves of a two-dimensional granular porous medium was simulated. Precipitation on grain surfaces occurred along a narrow zone in the middle of the domain, where the reacting solutes mixed to generate a supersaturated reaction product. The numerical simulations qualitatively reproduced the behavior observed in related laboratory experiments.

1. INTRODUCTION

It is generally recognized that fluid movement, mass transport and biogeochemical transformations that are observed at the field scale are related to molecular-, cellular- and pore-scale processes for which there is a growing body of scientific knowledge. However, high-resolution simulations of such detailed information cannot be carried out for complex, large-scale systems. The development of realistic and practical field-scale models will depend on a better understanding of how individual component processes are coupled, and better methods for passing information from micro-scale to continuum models. Physically based, broadly applicable computer models for micro-scale multiphase and multi-component fluid flow, solute transport and the growth/dissolution of solid phases in complex porous and fractured porous media are needed to develop a better understanding of a wide range of biogeochemical processes. In the past, grid-based (finite elements or finite difference) and lattice Boltzmann methods have been used to simulate small-scale (pore scale or fracture aperture scale) reactive flow in porous media. However, these methods are frequently plagued by artificial numerical diffusion, violation of mass conservation or lack of Galilean invariance, and they may suffer from numerical instabilities for large diffusion coefficients. The application of grid-based models is also complicated by geometrically complex boundaries that change dynamically as a result of precipitation, and the non-linearity of the flow and reactive transport equations.

In this paper, a Smoothed Particle Hydrodynamics (SPH) method is used to simulate pore-scale flow and reactive transport. The Lagrangian particle nature of SPH allows physical and chemical effects to be modeled with relatively little code-development effort. In addition, geometrically complex and/or dynamic boundaries and interfaces can be handled without undue difficulty. SPH was first introduced by Lucy (1977) and Gingold and Monaghan (1977) to simulate fluid dynamics in the context of astrophysical applications. SPH models have been successfully used to simulate a variety of subsurface process including micro-scale unsaturated (Tartakovsky and Meakin, 2005 a,b), saturated (Morris et al., 1997, Zhu et al.,

1999) and multiphase (Tartakovsky and Meakin, 2004, 2006) flows and non-reactive and reactive transport (Zhu and Fox, 2001, 2002, Tartakovsky and Meakin, 2005c, Tartakovsky et al., a, b) in fractured and porous media.

We extended the Tartakovsky et al. (a, b) model for precipitation from a supersaturated solution to simulate flow, mixing and reaction of two solutions, each containing single solutes (*A* and *B*) that react to form a product (*C*). The simulations results are compared with results of laboratory experiment in which Na_2CO_3 and $CaCl_2$ solutions were injected separately at the bottom of the different halves of a vertical 2-dimensional flow cell (Figure 2). Both numerical simulations and laboratory results show that precipitation occurs in a narrow zone along the interface between the two solutions.

2. SPH TRANSPORT EQUATIONS

There are a number of ways to represent the processes involved in precipitation that vary in terms of the level of detail and degree to which they correspond to known molecular and particle interactions. In this paper we have chosen to represent precipitation as heterogeneous growth of the reaction product (*C*) from a supersaturated solution. This approach is based on the idea that, providing the supersaturation index does not become too large, homogeneous nucleation will not occur, and precipitation will occur as overgrowth on pre-existing mineral surfaces. Future work will incorporate and test more explicit and detailed expressions for the kinetics of nucleation and growth. Fluid flow and solutes mixing and reaction of the type $A+B=C$ and precipitation of *C* can be described by a combination of the continuity equation,

$$d\rho / dt = \rho \nabla \cdot \mathbf{v}, \tag{1}$$

the linear momentum conservation equation,

$$d\mathbf{v} / dt = 1/\rho \nabla P + \mu / \rho \nabla^2 \mathbf{v} + 1/\rho \mathbf{F}^{ext}, \tag{2}$$

and the diffusion equations for species *A*, *B*, and *C* (Chopard et al., 1994),

$$dC^A / dt = D^A \nabla^2 C^A - k^{AB} C^A C^B, \tag{3}$$

$$dC^B / dt = D^B \nabla^2 C^B - k^{AB} C^A C^B, \tag{4}$$

$$dC^C / dt = D^C \nabla^2 C^C + k^{AB} C^A C^B, \tag{5}$$

where $\mathbf{v}$ is the fluid velocity, P is the fluid pressure, $\mathbf{F}^{ext}$ represents body forces (such as gravity acting on the fluid densities), μ is the fluid viscosity, ρ is the fluid density, C^A, C^B and C^C are the concentrations of a solutes *A*, *B* and *C* (the concentration is defined as the mass dissolved in a unit volume of fluid), D^A, D^B and D^C are the molecular diffusion coefficients of the corresponding species in the solvent and k^{AB} is a rate coefficient for $A + B = C$, normalized with respect to the equilibrium solubility product K_{sp}. For simplicity it is assumed that precipitation/dissolution of solute *C* is described by a first-order kinetic-reaction model at the fluid/solid interface:

$$D^C \nabla C^C \cdot \mathbf{n} = k(C^C - C_{eq}), \tag{6}$$

where C_{eq} is the concentration of *C* in equilibrium with solid *C*, $\mathbf{n}$ is the unit vector in the direction normal to the interface pointing toward the fluid and k is the local precipitation rate coefficient. The normal velocity, $\mathbf{v}_n$, at which the solid surface advances at position $\mathbf{x}_s$ on the fluid-solid interface into the liquid is given by

$$\mathbf{v}_n(\mathbf{x}_s) = D^C \nabla C^C(\mathbf{x}_s) \cdot \mathbf{n} / \rho_s , \tag{7}$$

where ρ_s is the density of the precipitated solid phase.

The SPH method is based on the idea that continuous field $A(\mathbf{r})$ can be approximated as $A_S(\mathbf{r}) = \sum_i A_i / n_i W(\mathbf{r} - \mathbf{r}_i)$ where W is the SPH weighting function, $\mathbf{r}_i$ is the position of particle i, $n_i = \rho_i/m_i$ is the particle number density, ρ_i and m_i are the fluid density and mass of particle i. The SPH approximation of continuous fields allows the mass and momentum conservation equations to be written in a form of a system of ordinary differential equations (ODEs) (Tartakovsky et al., 2005c),

$$n_i = \sum_j W(\mathbf{r}_j - \mathbf{r}_i) \qquad i, j \in \textit{fluid} + \textit{solid particles} \tag{8}$$

and

$$\frac{d\mathbf{v}_i}{dt} = -\frac{1}{m_i} \sum_{\substack{j \in fluid + \\ solid}} \left(\frac{P_j}{n_j^2} + \frac{P_i}{n_i^2} \right) \nabla_i W\left(\mathbf{r}_i - \mathbf{r}_j\right)$$

$$+ \frac{1}{m_i} \sum_{\substack{j \in fluid + \\ solid}} \frac{\left(\mu_i + \mu_j\right)\left(\mathbf{v}_i - \mathbf{v}_j\right)}{n_i n_j \left(\mathbf{r}_i - \mathbf{r}_j\right)^2} \left(\mathbf{r}_i - \mathbf{r}_j\right) \bullet \nabla_i W\left(\mathbf{r}_i - \mathbf{r}_j, h\right) + \frac{\mathbf{F}_i^{ext}}{m_i} . \qquad i \in \textit{fluid particles} \tag{9}$$

Both mobile fluids and solid boundaries are represented by particles. Particles representing solids are frozen in space but they enter into the calculation of forces acting on the fluid particles (eq. (9)). The velocities of the particles representing solid filled regions are set to zero and the number density of the fluid at the particle locations is found from equation (8).

Following Tartakovsky et al. (a, b) the system of diffusion/reaction equations (3)-(6) can be cast in the form of a system of ODEs:

$$\frac{dC_i^A}{dt} = \sum_{j \in fluid} \frac{D^A\left(n_i + n_j\right)\left(C_i^A - C_j^A\right)}{n_i n_j \left(\mathbf{r}_i - \mathbf{r}_j\right)^2} \left(\mathbf{r}_i - \mathbf{r}_j\right) \bullet \nabla_i W\left(\mathbf{r}_i - \mathbf{r}_j, h\right) - k^{AB} C_i^A C_i^B \tag{10}$$

$$\frac{dC_i^B}{dt} = \sum_{j \in fluid} \frac{D^B\left(n_i + n_j\right)\left(C_i^B - C_j^B\right)}{n_i n_j \left(\mathbf{r}_i - \mathbf{r}_j\right)^2} \left(\mathbf{r}_i - \mathbf{r}_j\right) \bullet \nabla_i W\left(\mathbf{r}_i - \mathbf{r}_j, h\right) - k^{AB} C_i^A C_i^B \tag{11}$$

and

$$\frac{dC_i^C}{dt} = \sum_{j \in fluid} \frac{D^C\left(n_i + n_j\right)\left(C_i^C - C_j^C\right)}{n_i n_j \left(\mathbf{r}_i - \mathbf{r}_j\right)^2} \left(\mathbf{r}_i - \mathbf{r}_j\right) \bullet \nabla_i W\left(\mathbf{r}_i - \mathbf{r}_j, h\right)$$

$$+ k^{AB} C_i^A C_i^B - R \sum_{k \in solid} \left(C_i^C - C_{eq}\right) \delta_{ik} \tag{12}$$

where C^I_i is the concentration of the solute I at fluid particle i, R is the effective "particle" fluid-solid reaction rate constant, $\sum_{j \in fluid}$ indicates summation over all the fluid particles, $\sum_{k \in solid}$ indicates summation over all the solid particles and $\delta_{ik} = 1$ if $\left|\mathbf{r}_i - \mathbf{r}_k\right| \le d$ and zero otherwise. The effective "particle" fluid-solid reaction rate is given by $k \approx RdN^{\text{int}}$, where N^{int},

the average number of fluid particles that interact with each solid particle, depends on the particle number density, d and, in general, the particle radial distribution function, g(r). Precipitation and dissolution are modeled by tracking the masses, m_i, of the solid particles, which change according to:

$$\frac{dm_i}{dt} = R\sum_{j\in f}\frac{1}{n_j}\left(C_j - C_{eq}\right)\delta_{ij} \qquad i \in s\,. \tag{13}$$

Once the mass of a solid particle reaches twice the original mass, m_0, the nearest fluid particle 'precipitates', becoming a new solid particle, and the masses of both the new and old solid particles are set to m_0. Similarly, if the mass of a solid particle reaches zero, the solid particle becomes a new fluid particle. Since the new fluid particles will be very close to the solid boundary, where the fluid velocity is very small, the initial velocity of a new fluid particle is set to zero.

2.1 Implementation of the SPH model.

At each time step in a simulation, the particle number densities, $n_{i,}$ at each of the particles are calculated using equation (8) and the pressure at each particle is obtained using the equation of state $P_i = P_{eq}n_i/n_{eq}$. Then the right hand side of equation (9) is evaluated and new concentrations are calculated. Particle accelerations, $\mathbf{a}_i = d\mathbf{v}_i/dt$, are found from equation (9), and fluid particle velocities, positions and concentrations are found by integrating the SPH equation of motion using the explicit "velocity Verlet" algorithm (Allen and Tildesley, 2001). An M_6 spline function (Schoenberg, 1946) was used for the SPH smoothing function.

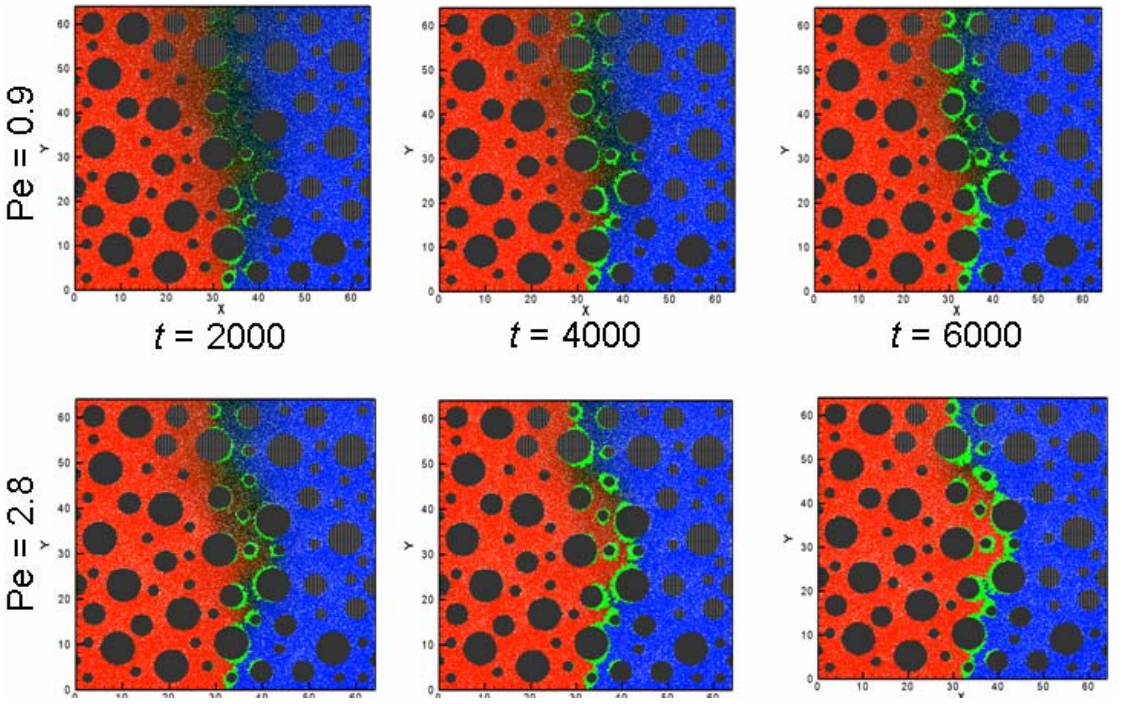

FIGURE 1. Flow and precipitation for two Peclet numbers.

3. NUMERICAL RESULTS AND LABORATORY EXPERIMENT

Figure 1 shows simulations of the mixing of two reactive fluids and mineral precipitation in the porous medium for two different Peclet numbers. The solutes *A* (red particles) and *B* (blue particles) were injected at the same rate into the right and left parts of the computational domain. As the solutions mix, *A* and *B* react according to equations (3)-(5) and produce *C*, which precipitates on mineral surfaces according to equation (6). The black particles represent the distribution of dissolved *C*, the gray particles represent mineral grains and the green particles are precipitated solid *C*.

To initialize the simulations, particles were placed randomly into a 64 × 64 box (in units of *h*), and the SPH equation (9), with $\mathbf{F}^{ext} = 0$, and periodic boundary conditions in all directions were used to bring the system into an equilibrium state. The equilibrium particle density was $n_{eq} = 16\ h^{-2}$ (16 particles in an area of h^2). The coefficient P_{eq} in the equation of state was $P_{eq} = 20$ and the viscosity was $\mu_i = 1$. After equilibrium was reached, the particles at positions $\mathbf{x}_i$ covered by the discs used to represent solid grains were 'frozen' to form impermeable boundaries to the flow. After the fluid particles were identified, each fluid particle was assigned A and B concentration of zero and a *C* concentration of *Ceq*. A body force was then applied in the *y* direction. No flow boundary conditions were imposed at the soil grain boundaries and at the boundaries of the computational domain in the x direction, and periodic flow boundary conditions were used in the *y* direction. Particles exiting the flow domain at y = 64 were returned into the flow domain at $x = 0$. The concentrations C_A=1, C_B = 0, $C_C = C_{eq}$ (C_{eq} = 0.15) were assigned to the particles entering at $y = 0$ in the left part of domain and C_A=0, C_B = 1, $C_C = C_{eq}$ in the right part of domain. Mixing of the solutes *A* and *B* and subsequent formation of the species *C* occurs only in the narrow zone in the middle of the domain. The width of this zone is practically independent of the Peclet number, Pe, but the concentration of *C* increases with increasing Pe. The mixing zone decreases with time as precipitate reduces contact between solutes *A* and *B*. The fluid velocity field is not affected significantly by precipitation as precipitation occurs mainly in a narrow zone in the direction of flow.

The numerical results qualitatively agree with results of laboratory experiments. Two solutes (Na_2CO_3 and $CaCl_2$) were injected at the bottom of the vertical 2-dimensional flow cell as shown on the Figure 2. The fluid cell was approximately 60 cm high and 60 cm wide.

FIGURE 2. Na_2CO_3 and $CaCl_2$ solutions injected separately at the bottom of the different halves of a vertical 60cm x 60 cm flow cell. The white line in the middle of flow cell is a zone of calcium carbonate precipitation.

The white line in the middle of the flow cell is a zone of calcium carbonate precipitation produced by reaction of Na_2CO_3 and $CaCl_2$. Despite the fact that equations (3) – (6) provide only a caricature of the calcite precipitation process (there is no intermediate reaction product, C, in the experimental system), precipitation occurs only in the narrow zone along the interface between the two solutions in both the experiments and simulations. On the other hand, Darcy scale simulations of this experiment using continuum model code such as HYDROGEOCMEM (Yeh et al., 2004) predicted a significantly wider precipitation zone. The reason for the failure of the continuum model is that mixing and precipitation in the experiment is very localized and produces high concentration gradients in a region that is only several soil grains wide. This may lead to the failure of advective dispersion models based on the local averages.

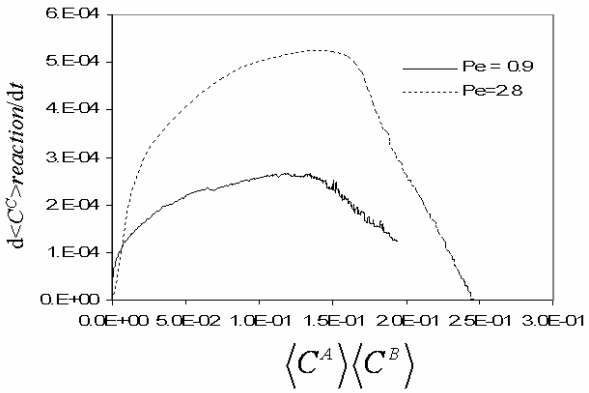

FIGURE 3. Rate of change of $<C^C>$ due to reaction between solutes *A* and *B* versus the product of the average concentrations $<C^A><C^B>$ for two Peclet numbers.

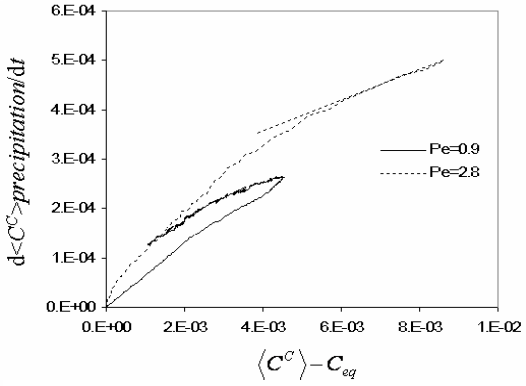

FIGURE 4. Rate of change of $<C^C>$ due to precipitation as a function of $<C^C>$ - C_{eq} for two Peclet numbers.

Figure 3 shows the rate of change of the average solute *C* concentration, $\langle C^C \rangle$ due to reaction between solutes *A* and *B* versus the product of the average concentrations $<C^A><C^B>$ as a function of Pe. The concentration of *i-th* solute averaged over the entire pore volume of the computational domain, *V*, is given by $\langle C^I \rangle = \int_V C^I(\mathbf{x})d\mathbf{x}/V \approx \sum_{i \in \text{fluid particles}} C_i^I / N_f$. It can be seen that the reaction producing solute *C* is not linear with respect to $<C^A><C^B>$. This figure also shows that averaging of the concentrations over a volume (even one as small as that used in the SPH simulations) may lead to erroneous results. At late times during injection, when the formation of precipitates significantly limits direct contact and mixing between solutes *A* and *B*, the rate of production of $<C^C>$ decreases with increasing $<C^A><C^B>$, while the dC_i^C/dt linearly increases with increasing $C^A{}_i C^B{}_i$ at the position of particle *i* according to equation (5). Figure 4 shows the rate of change of $<C^C>$ due to precipitation as a function of $<C^C>$ - C_{eq} for two Peclet numbers. This figure indicates that the effective precipitation rate (slope of the curve) is defined in two distinct branches. The lower branch corresponds to the first part of the simulation during which the solute concentration increases as the mixing zone of solutes *A* and *B* develops. The upper branch corresponds to the second part of the simulations during which pore filling due to precipitate formation reduces mixing between *A*

and *B*. The complex behavior indicates that the effective reaction rate coefficient depends on the local history of the reactive transport process. It can be also seen that effective precipitation rate increases with increasing Peclet number.

4. CONCLUSIONS

Laboratory experiments were performed to investigate the injection of reactive solutions into different halves of a quasi two-dimensional porous medium, and the experiment was simulated using a two-dimensional model. Mixing of the solutes *A* and *B* and subsequent precipitation of the solute *C* was observed in a narrow zone in the middle of domain. The width of this zone was found to be practically independent of the Peclet number, but the precipitation rate increased with increasing Pe. The mixing zone decreased with time as precipitated minerals reduced contact between solutes *A* and *B*. The simulations and experiments lead to similar results because in both precipitation occurs most rapidly in regions in which the solute concentration product $C^A C^B$ is largest and the removal of A and B due to reaction or precipitation is essentially irreversible.

The precipitation greatly effects mixing of the two solutes, and this illustrates why the simple continuum-scale model does not properly predict the width of the reaction zone. It is possible that, by using a very highly-resolved numerical grid in the mixing zone and incorporating the reactions in the continuum model (including changes in diffusion rates associated with precipitation), the continuum model might adequately predict the macroscopic precipitation features shown in Figure 2. We are performing further numerical studies to test this hypothesis. As an alternative, we are also exploring the integration of pore- and continuum-scale models directly using a hybrid modeling approach. In this approach, the pore-scale SPH model will be used to simulate flow, transport, and reaction in the small portion of the experimental domain corresponding to the mixing zone, and the continuum-scale reactive transport model will be used for the remainder of the experimental domain (where local mixing and reactions are insignificant). This approach has been successfully applied to other problems in which highly localized processes manifest themselves in macroscopic phenomena in complex ways (for example, microfracture propagation in materials science). We believe that, for porous media problems that involve strong coupling between flow, transport, and reaction processes, a hybrid model approach will not only have computational advantages, but will also provide a more fundamentally sound representation of the underlying physics and chemistry of the system.

ACKNOWLEDGEMENTS

This research was supported by the Laboratory Directed Research and Development program at the Pacific Northwest National Laboratory and the Environmental Management Science Program of the Office of Science, U.S. Department of Energy. The Pacific Northwest National Laboratory is operated for the U.S. Department of Energy by Battelle under Contract DE-AC06-76RL01830, and the Idaho National Laboratory is operated for the U.S. Department of Energy by the Battelle Energy Alliance under Contract DE-AC07-05ID14517.

REFERENCES

Allen, M. P., and D. J. Tildesley (2001), Computer simulation of liquids, Oxford University Press, Oxford, 81

Chopard, B., P. Luthi, and M. Droz (1994), Reaction-Diffusion Cellular Automata Model for the Formation of Liesegang Patterns, Phys. Rev. Let., 72(9) 1384

Gingold, R. A., and J. J. Monaghan (1977), Smoothed particle hydrodynamics: theory and application to non-spherical stars, Monthly Notices of the Royal Astronomical Society, 181, 375.

Lucy, L. B. (1977), Numerical approach to the testing of the fission hypothesis, Astronom. J., 82, 1013.

Morris, J. P., P. J. Fox, and Y. Zhu (1997), Modeling low Reynolds number incompressible flows using SPH, J. Comput. Phys., 136, 214.

Schoenberg, I. J. (1946), Contributions to the problem of approximation of equidistant data by analytical functions: part A, Q. Appl. Math. IV 45.

Tartakovsky, A. M., and P. Meakin (2004), Application of smoothed particle hydrodynamics to the simulation of multiphase flow in complex fractures, International conference "Computational Methods in Water Resources", Chapel Hill, North Carolina USA, June 13-17.

Tartakovsky, A. M., and P. Meakin (2005a), Modeling of surface tension and contact angles with smoothed particle hydrodynamics, Phys. Rev. E, 72, 026301.

Tartakovsky, A. M., and P. Meakin (2005b), Simulation of free-surface flow and injection of fluids into fracture apertures using smoothed particle hydrodynamics, Vadose Zone J., 4, 848.

Tartakovsky, A. M., and P. Meakin (2005c), A smoothed particle hydrodynamics model for miscible flow in three-dimensional fractures and the two-dimensional Rayleigh-Taylor instability, J. Comput. Phys., 207, 610.

Tartakovsky, A. M., and P. Meakin (2006), Pore-scale modeling of immiscible and miscible fluid flows using smoothed particle hydrodynamics, (in press)

Tartakovsky, A. M., P. Meakin, and T. Scheibe (a), Simulations of reactive transport and precipitation with smoothed particle hydrodynamics, J. Comput. Phys., under review.

Tartakovsky, A. M., P. Meakin, and T. Scheibe (b), A smoothed particle hydrodynamics model for reactive transport and mineral precipitation in porous and fractured porous media, Water Resour. Res., under review.

Yeh, G. T., J. T. Sun, P. M. Jardine, W. D. Burgos, Y. L. Fang, M. H. Li, and M. D. Siegel (2004), HYDROGEOCHEM 5.0: A three-dimensional model of coupled fluid flow, thermal transport and hydrogeochemical transport through variable saturated conditions -- Version 5.0, Technical report ORNL/TM-2004/107, Oak Ridge National Laboratory, Oak Ridge, TN.

Zhu, Y., P. J. Fox, and J. P. Morris **(**1999), A pore-scale numerical model for flow through porous media, Int. J. Num. Analyt. Meth. Geomech., 23, 881.

Zhu, Y., and P. J. Fox (2001), Smoothed particle hydrodynamics model for diffusion through porous media, Transp. in Porous Media, 43, 441.

Zhu, Y., and P. J. Fox (2002), Simulation of pore-scale dispersion in periodic porous media using smoothed particle hydrodynamics, J. Comput. Phys., 182, 622.